Tectonophysics 526–529 (2012) 5–15

Contents lists available at SciVerse ScienceDirect

Tectonophysics

journal homepage: www.elsevier.com/locate/tecto

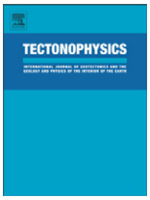

Unraveling topography around subduction zones from laboratory models

Laurent Husson [a,b,*], Benjamin Guillaume [a,b,c,d], Francesca Funiciello [d], Claudio Faccenna [d], Leigh H. Royden [e]

[a] CNRS UMR6118, Geosciences Rennes, Universite de Rennes 1, Rennes, France
[b] CNRS UMR 6112, LPG Nantes, Universite de Nantes, Nantes, France
[c] CNR, Istituto di Geologia Ambientale e Geoingegneria, Rome, Italy
[d] Dipartimento di Scienze Geologiche, Universita Roma Tre, Rome, Italy
[e] Department of Earth, Atmospheric and Planetary Sciences, Massachusetts Institute of Technology, Cambridge, MA 02139, USA

ARTICLE INFO

Article history:
Received 7 January 2011
Received in revised form 1 July 2011
Accepted 6 September 2011
Available online 7 November 2011

Keywords:
Subduction
Dynamic topography
Dynamic pressure
Forebulge
Analog modeling

ABSTRACT

The relief around subduction zones results from the interplay of dynamic processes that may locally exceed the (iso)static contributions. The viscous dissipation of the energy in and around subduction zones is capable of generating kilometer scale vertical ground movements. In order to evaluate dynamic topography in a self-consistent subduction system, we carried out a set of laboratory experiments, wherein the lithosphere and mantle are simulated by means of Newtonian viscous materials, namely silicone putty and glucose syrup. Models are kept in their most simple form and are made of negative buoyancy plates, of variable width and thickness, freely plunging into the syrup. The surface of the model and the top of the slab are scanned in three dimensions. A forebulge systematically emerges from the bending of the viscous plate, adjacent to the trench. With a large wavelength, dynamic pressure offsets the foreside and backside of the slab by ~500 m on average. The suction, that accompanies the vertical descent of the slab depresses the surface on both sides. At a distance equal to the half-width of the slab, the topographic depression amounts to ~500 m on average and becomes negligible at a distance that equals the width of the slab. In order to explore the impact of slab rollback on the topography, the trailing edge of the plates is alternatively fixed to (fixed mode) and freed from (free mode) the end wall of the tank. Both the pressure and suction components of the topography are ~30% lower in the free mode, indicating that slab rollback fosters the dynamic subsidence of upper plates. Our models are compatible with first order observations of the topography around the East Scotia, Tonga, Kermadec and Banda subduction zones, which exhibit anomalous depths of nearly 1 km as compared to adjacent sea floor of comparable age.

1. Introduction

Topography results from a variety of processes that, particularly near subduction zones, exhibit strong spatial gradients. At the surface of the Earth, the conjunction of these processes not only produces deviations from the geoid (such as over the deep sea trenches), but also the largest topographic slopes that exist offshore and onshore. The topographic expression of subduction zones consists as the juxtaposition of a depressed bathymetry of the overriding plate, a deep trench in front of the overriding plate, and an outer rise (or forebulge). This structure correlates well with the gravity signal, in particular long wavelength geoid highs that correspond to the density anomalies of the subducted slabs, overprinted by sharp free air lows over the trenches that highlight the dynamic nature of the topographic depression, and an intermediate scale free air low that highlights the dynamic deflection of the overriding plate (Husson, 2006; Melosh and Raefsky, 1980; Morgan, 1965; Watts and Talwani, 1974; Zhong and Gurnis, 1992).

The processes that generate the total relief can be separated into the static components, that are primarily due to the lateral density variations within the lithosphere, and the more elusive dynamic topography that is, within its common geophysical sense, the response of the surface to the stresses that arise from the underlying mantle flow (Čadek and Fleitout, 2003; Colin and Fleitout, 1990; Conrad and Husson, 2009; Moucha et al., 2008). The process is well known in theory, and a body of work has focused on explaining a variety of transgressive episodes *via* models of dynamic topography around subduction zones (Boschi et al., 2010; Faccenna and Becker, 2010; Gurnis, 1990b, 1992; Husson, 2006; Liu et al., 2008; Mitrovica, 1996; Spasojevic et al., 2009). However, the magnitude and wavelength of dynamically maintained topographic anomalies remains highly uncertain (see *e.g.* Krien and Fleitout (2008)). Even if many of the cited applications are appealing, Wheeler and White (2000) conversely found no significant dynamic topography in South East Asia, where dynamic topography

---

* Corresponding author at: CNRS UMR6118, Geosciences Rennes, Universite de Rennes 1, Rennes, France. Tel.: +33 223236080.
E-mail address: lhusson@univ-rennes1.fr (L. Husson).

0040-1951/$ – see front matter © 2011 Elsevier B.V. All rights reserved.
doi:10.1016/j.tecto.2011.09.001

above the many subducted slabs should be well developed. Uncertainty persists for several reasons.

First, the observation of the topography of the Earth around subduction zones is blurred by the convolution of complex mechanisms that produce the topography, and therefore requires meticulous analysis of the topography and gravity signals (Billen and Gurnis, 2005). But only a clear conception of the structure of the lithosphere at a global scale, and at a degree that is almost always beyond our current knowledge, could definitely solve this issue. Second, confusion may arise from the definition of dynamic topography. In fact, several components of the topography have a dynamic origin, and attributing it to the sole contribution of mantle flow underneath the lithosphere is restrictive. In particular around subduction zones, a variety of dynamic processes lead to the formation of the forebulge and the trench. Third, a variety of studies have individually explored the different mechanisms, predicting a plausible relief that integrates most subduction processes within dedicated numerical models, even in three dimensions. However, at this stage, many technical challenges (free surface condition, three-dimensional aspect) or mechanical issues (one-sided subductions, trench behavior, *etc*…) make numerical simulations around subduction zones not definitive. In fact, only few attempts have been made to capture all the elements of the topography around subduction zones together (Billen et al., 2003; Buiter et al., 2001; Melosh and Raefsky, 1980; Zhong and Gurnis, 1992).

Analog models may offer an alternative. In this paper, we build upon classic analog models of subduction zones (Bellahsen et al., 2005; Funiciello et al., 2003; Schellart, 2004) to unravel the topography around subduction zones. The following experiments therefore represent a first attempt to reproduce the topography around subduction zones self-consistently, *i.e.* by examining the case of *free* subductions, wherein the dynamics is only driven by the buoyancy of the slab and resisted by the viscous flow in the surrounding mantle.

2. The models

2.1. Experimental setup

We carried out a set of 13 experiments that essentially reproduce the lines of the experiments of Bellahsen et al. (2005) or Funiciello et al. (2003) (Supplementary material 1). We use silicone putty (Rhodrosil Gomme, PDMS, iron fillers) and glucose syrup to model the lithosphere and the upper mantle, respectively. Silicone putty is a viscoelastic material but its Maxwell time (<1 s) precludes any elastic behavior in our models lasting tens of minutes. Glucose syrup is a transparent Newtonian low-viscosity and low-density fluid, compared to the silicone putty. These materials have been selected to achieve the standard scaling procedure for stresses scaled down for length, density and viscosity in a natural gravity field (Davy and Cobbold, 1991; Weijermars and Schmeling, 1986).

The scale factor for length is 1.5×10^{-7} (1 cm in the experiment corresponds to 66 km in nature) (Table 1). Densities and viscosities are assumed to be uniform over the thickness of the individual layers and are considered to be averages of the actual values. For the reference model, described hereafter, the negative buoyancy of the lithosphere is -91 kg/m^3 (Table 1). The range of possible density contrast relies on several hypothesis regarding the age–buoyancy and nature of the subducting lithosphere. Alternatively, Doglioni et al. (2007) suggest that slabs may not be negatively buoyant but are instead pushed into the mantle by the flowing mantle itself. The viscosity ratio between the slab and the surrounding mantle (η_l/η_m) is 1.4×10^4. This value is an upper bound in the range of what we consider possible natural values (Billen et al., 2003; Funiciello et al., 2008; Loiselet et al., 2009; Wu et al., 2008), although alternative views suggest higher viscosity ratios (Doglioni et al., 2007).

Table 1
Scaling of the modeling parameters in nature and in the laboratory, for the reference model.

	Parameters		Nature	Reference model
g	Gravitational acceleration	m/s^2	9.81	9.81
Length				
W	Subducting plate width	m	990,000	0.15
H	Subducting plate thickness		100,000	0.0152
D	Upper mantle thickness		660,000	0.10
	Scale factor for length		$L_{\mathrm{model}}/L_{\mathrm{nature}} = 1.52 \times 10^{-7}$	
Buoyancy				
$\rho_m - \rho_l$	Subducting oceanic plate	kg/m^3	-80 (80 Myr-old plate)	-91
	Scale factor for buoyancy		$\Delta\rho_{\mathrm{model}}/\Delta\rho_{\mathrm{nature}} \simeq 1$	
Viscosity				
η_l	Subducting oceanic plate	Pas	1.4×10^{24}	4.2×10^5
η_m	Upper mantle		10^{20}	30
	Scale factor for viscosity		$\eta_{\mathrm{model}}/\eta_{\mathrm{nature}} = 3 \times 10^{-19}$	
Characteristic time				
t	$t_{\mathrm{nature}}/t_{\mathrm{model}} = ((\Delta\rho g H)_{\mathrm{model}}/(\Delta\rho g H)_{\mathrm{nature}}) \times (\eta_{\mathrm{nature}}/\eta_{\mathrm{model}})$	s	3.16×10^{13} (1 Myr)	55
	Scale factor for time		$t_{\mathrm{model}}/t_{\mathrm{nature}} = 1.74 \times 10^{-12}$	

2.2. Experimental procedure

The system is disposed in an 80 cm wide square tank (Fig. 1). The experimental subduction is started by manually forcing the leading edge of the silicone plate into the glucose downward to a depth of 3 cm (corresponding to about 200 km in nature). We used a 3D laser scanner above the tank and digitized the deforming topography, with a maximum horizontal resolution of 0.13 mm. The precision of punctual topographic data is 0.05 mm, which considerably improves when a statistical treatment is applied. In the following, we refer to the side of the unsubducted portions of the plate as the foreside and conversely, the backside is the region above the sunken slab (Fig. 1).

For modeling convenience, each experiment is separated into two sub-experiments. The first stage of the experiments takes place within the framework of *fixed edge* subduction *sensu* Kincaid and Olson (1987), *i.e.* the trailing edge of the slab is attached to the tank in order to preclude any trenchward motion of the silicone plate. When steady state is reached (when the generic *S* shape of the retreating slab is reached and the geometry remains unchanged in the referential of the moving trench), the shape of the silicone slab is scanned before the surface is spray-painted (in order to overcome optical issues due to the translucency of the glucose syrup) and scanned as well. When all measurements are done, the trailing edge of the silicone slab is freed from the tank, and the subduction enters a *free edge* mode for a second sub-experiment. Because the surface remains painted from the first stage, it is technically impossible to scan the surface of the slab at depth without strongly damaging the experiment. Only the topography of the surface of the model is thus acquired when a new steady state is reached.

2.3. Force balance

Our simplified subduction system is designed in order to impose a straightforward force balance that approximately reproduces that of